Electronic and magnetic structure of cuprous oxide Cu$_2$O doped with Mn, Fe, Co, and Ni: A density-functional theory study

M. Sieberer, J. Redinger, and P. Mohn

Center for Computational Materials Science, Vienna University of Technology, Getreidemarkt 9/134, A-1060 Vienna, Austria

We investigate the effect of transition metal (TM) substitution in cuprous oxide Cu$_2$O on the basis of *ab initio* calculations employing density-functional theory (GGA+U). By using the supercell approach, we study the effect of substituting Cu by Mn, Fe, Co, and Ni, assuming both low TM concentrations (3.2%) in a cubic geometry and higher TM concentrations (9.1%) in a trigonal setup. For the elements Mn and Co, magnetic exchange constants up to the fifth nearest neighbor are calculated, assuming both cases, perfect Mn/Co:Cu$_2$O as well as defects in the host such as single copper and oxygen vacancies. Our results clearly show the importance of defects in these materials and thus offer an explanation for various, seemingly opposed, experimental results.

I. INTRODUCTION

There is considerable interest in diluted magnetic semiconductors, especially with emphasis on the exploration of suitable semiconductor hosts. A rather different family, namely the oxide-based diluted magnetic semiconductors, are attracting increasing attention, following reports of room temperature ferromagnetism in anatase TiO$_2$ and wurtzite ZnO doped with a range of transition metal ions. In this paper we explore a new suitable host, namely cuprous oxide (Cu$_2$O), which has already been prepared with a small concentration of Mn, Co, and Ni on the copper sites. In Mn-doped Cu$_2$O, the experimental results disagree in the context of room temperature ferromagnetism,[1–3] in the Co-doped compound only the results of Kale *et al.*[4] are available, pointing towards room temperature ferromagnetism if in addition Al codoping is performed. On the theoretical side, Ag, Ni, and Zn doping have been investigated,[5] but magnetic properties were not mentioned. Thus we study Mn, Fe, Co, and Ni inserted in Cu$_2$O by the means of density-functional theory (GGA and GGA+U) using the VASP code. By setting up 48-atom supercells ($2\times2\times2$ fcc cells) as well as 18-atom trigonal cells (simplest trigonal unit cells) with one or two copper atoms being replaced, we are already within the experimental doping regime. Correlations beyond GGA as well as geometrical relaxations around the impurity are taken into account. We analyze energy differences between ferromagnetic and antiferromagnetic coupling of spins situated on the substituents Co and Mn, in order to obtain better insights into the magnetic exchange mechanisms in these compounds.

II. COMPUTATIONAL METHOD

The calculations were performed using the VASP package,[6] which implements a plane-wave basis and a projector augmented wave (PAW) technique.[7] Exchange and correlation were treated within the density functional formalism[8] using the generalized gradient approximation of Perdew, Burke, and Ernzerhof.[9] Effects of electron correlation beyond GGA were taken into account within the framework of GGA+U.

To this end, the simplified (rotationally invariant) approach of Dudarev has been used.[10] Since no data from spectroscopic measurements were available, values of $U=5$ eV and $J=0.95$ eV have been applied for Mn, Fe, Co, and Ni. PAW potentials have been used, with $4s$, $3d$, and $4p$ electrons in valence for copper and $2s$ and $2p$ electrons in valence for oxygen. A plane-wave expansion up to 400 eV was sufficient. For the supercell calculations (48 atoms) a **k** mesh of $8\times8\times8$ within the full Brillouin zone has been used, except in the cases where symmetry constraints were switched off a $6\times6\times6$ mesh has been utilized. For the trigonal cells, a **k** mesh of $18\times18\times14$ within the full Brillouin zone turned out to yield good results.

III. PURE CUPROUS OXIDE

Cuprous oxide (Cu$_2$O) is a *p*-type semiconducting oxide with a direct band gap of approximately 2.1 eV (Ref. 11) that crystallizes in a cubic structure (Pn$\bar{3}$m, No. 224) built up from Cu atoms located on a conventional fcc lattice and oxygens at the positions $\left(\frac{1}{4},\frac{1}{4},\frac{1}{4}\right)$ and $\left(\frac{3}{4},\frac{3}{4},\frac{3}{4}\right)$. While the coppers are linearly (twofold) coordinated, the oxygens are situated in the center of ideal tetrahedra (Fig. 1). This structure may also be viewed as consisting of two independent and interpenetrating O-Cu-O zigzag frameworks, each one equivalent
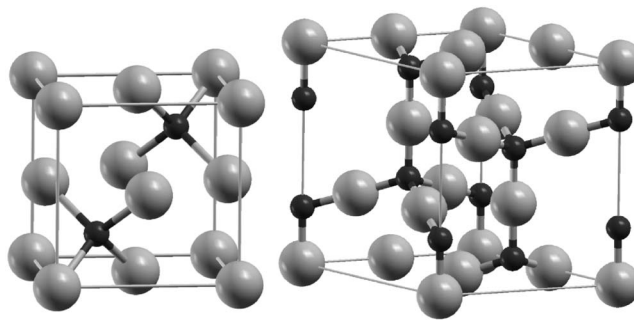
FIG. 1. Left panel: Cubic unit cell of Cu$_2$O containing six atoms. The big bright spheres are Cu atoms, the small dark ones are oxygens. Right panel: Trigonal unit cell Cu$_{12}$O$_6$.
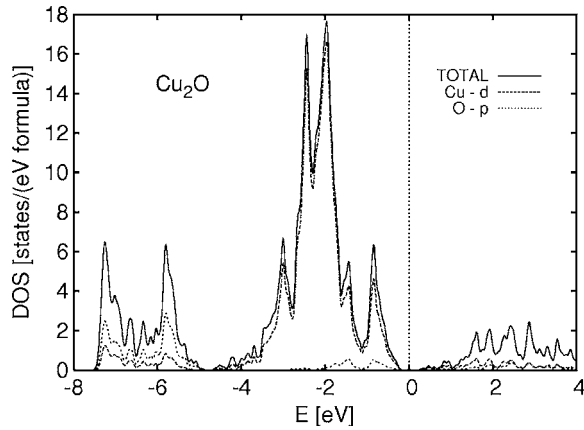
FIG. 2. Density of states for Cu_2O.

to the cristobalite structure. The calculated lattice constant is 8.14 a.u., in good agreement with the experimentally found lattice constant of $a_0 = 8.07$ bohr.[12] The calculated gap is too small (0.48 eV), but otherwise—due to the formally fully occupied 3*d* shell—one expects band theory to give good results. This has been confirmed by Ghijsen *et al.*[13] by performing several types of spectroscopies. Laskowski *et al.*[14] found out that local-density approximation (LDA) as well as GGA slightly overestimate the *s-d* hybridization, but this effect can be assumed to play a minor role in the following discussion.

The density of states (DOS) of Cu_2O is shown in Fig. 2. In addition to the total DOS per formula unit, Cu-*d* and O-*p* states are shown. The DOS below E_F has mainly three features, a main Cu *d* block situated at ≈ -2 eV, a broad oxygen *p* peak around ≈ -7 eV, and one narrow peak at the upper edge of the Cu *d* block, which is mainly built up from Cu d_{z^2}, d_{xz}, and d_{yz} orbitals. One of the reasons for the stability of Cu_2O is its incompletely filled d_{z^2} orbital. In the Orgel model[15] this is justified by the formation of a s-d_{z^2} hybrid orbital on Cu, resulting in the tendency to occupy Cu *s*-like states and to emtpy (antibonding) Cu d_{z^2} states. More detailed discussions on the electronic structure of Cu_2O can be found, e.g., in Refs. 16–19.

IV. TRANSITION METAL SUBSTITUTION

Experimentally much effort was put into the preparation of transition metal doped Cu_2O. At the moment there is some

controversy about room temperature ferromagnetism in Mn doped Cu_2O. Wei *et al.*[1] reported a T_c of more than 300 K for bulk Cu_2O and thin films if doped with 1.7% of Mn, whereas Pan *et al.*[2] identified only paramagnetic behavior. For higher doping (nominal $Cu_{1.9}Mn_{0.1}O$) Ivill *et al.*[3] reported no magnetic signal except that of a ferromagnetic Mn_3O_4 impurity phase with a T_c of ≈ 46 K. Also, Co-doped thin films were prepared, room temperature ferromagnetism was indeed reported, but only if 0.5% Al were co-doped,[4] otherwise some hints pointing towards spin-glass behavior were found. Ni-doped films were also synthesized,[20] but without analyzing their magnetic properties. Even though band-structure calculations for Ag-, Ni-, and Zn-doped Cu_2O with a rate of substitution of 12.5% were done,[5] nothing is known about more dilute systems and about magnetism.

A. Relaxations

In order to be close to experimental doping concentrations, supercells containing 48 atoms (eight fcc cells with six atoms each) have been set up, assuming the transition metal (TM) to be located at the origin. This is equivalent to a substitution of 3.125% of the copper atoms and yields a TM-TM distance of 8.614 Å. For a realistic description of $TM_1Cu_{31}O_{16}$, in VASP all symmetry (D_{3d}) conserving relaxations have been taken into account. The ionic degrees of freedom were converged better than 1 meV, all forces better than at least 0.06 eV/Å. The lattice constant has been fixed at the (GGA) optimized value of the host material (16.28 a.u.), and from now on will be used in all calculations. In Table I the relative changes in the bond length as compared to the pure Cu_2O host as well as the relative changes in the TM-Cu distance (fcc nearest neighbor sites) are listed. For $U=0$ all calculations agree that the nearest neighbor relaxations are most important for Mn and Co, but only small for Fe and Ni. In all cases the Cu ions come closer to the substituent and it is found that this relaxation is strongest for Co and Fe. This feature is reasoned by the deviation from the d^{10} configuration, which causes stronger TM-Cu bonds. There is a clear trend towards a strengthening of the bond between TM-O and TM-Cu for both $U=0$ and $U=5$ eV when going from Mn to Co, but a weakening of the bond for Ni. A finite Hubbard U always leads to an increase of the bond length, which is a consequence of the localization of the *d* states which prevents them from participating in the chemical bond. The fact that the Co-O bond length is shortest can be explained by the approximately half-filled $d^{\downarrow}$

TABLE I. Δr_{NN} denotes the changes in the TM-O bond length relative to the pure host, d/d_{ideal} is the relative change of the TM-Cu distance, equivalent to nearest neighbor sites in an fcc lattice.

	Mn	Fe	Co	Ni
$U=0$, 48 atoms				
Δr_{NN} [%]	+2.5	+0.4	−1.2	+0.5
d/d_{ideal} [%]	−0.74	−1.26	−1.50	−1.11
$U=5$ eV, 48 atoms				
Δr_{NN} [%]	+5.2	+2.3	+0.6	+2.6
d/d_{ideal} [%]	+1.91	−0.35	−0.12	+1.37
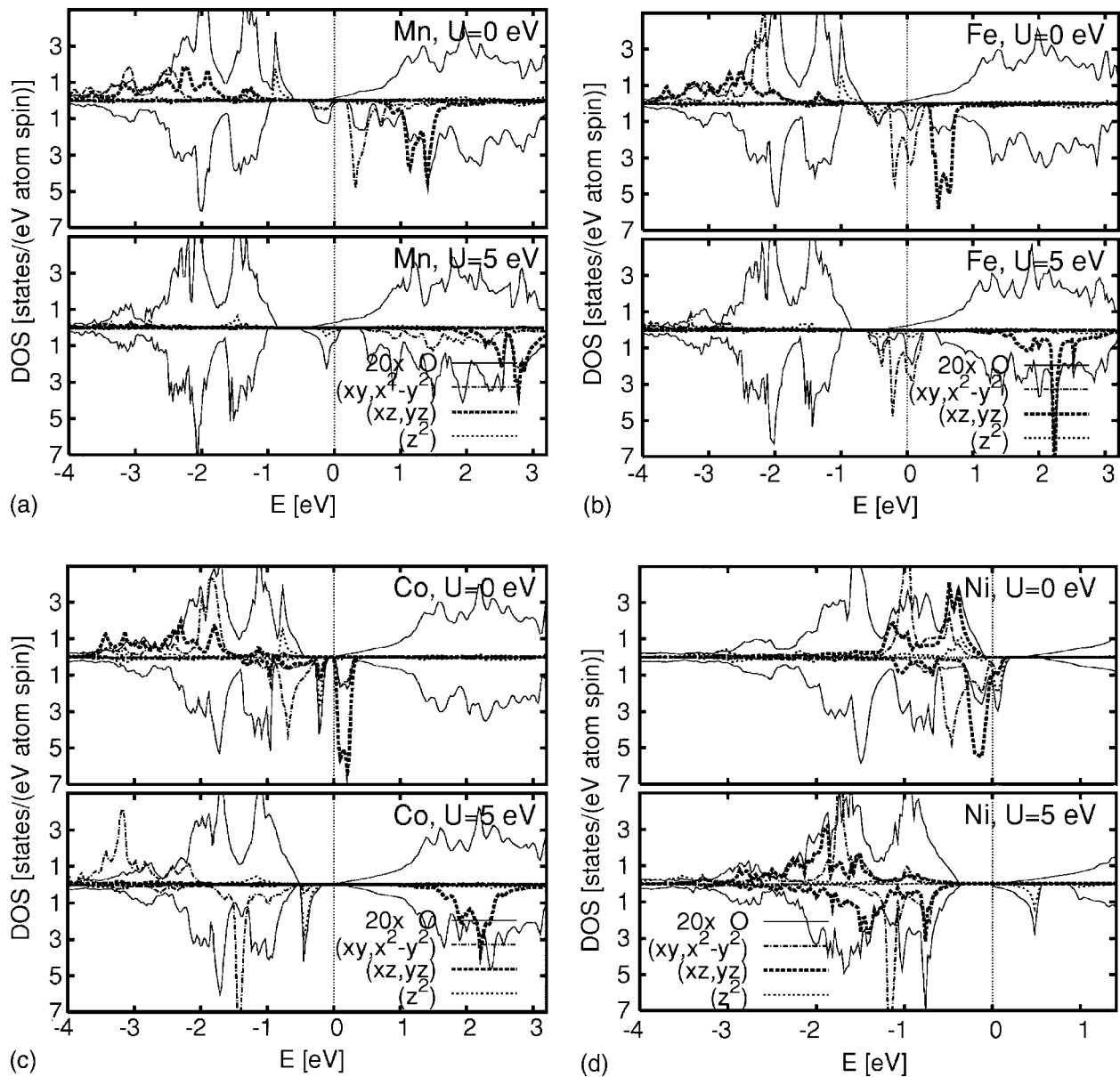
FIG. 3. Density of states (DOS) for $TM_1Cu_{11}O_6$ with TM=Mn (a), Fe (b), Co (c), and Ni (d). The TM d-like DOS (radius of integration: r_{TM}=2.5 bohr) is splitted in its irreducible representations, and the total DOS of oxygen (r=1.55 bohr) has been multiplied by 20. One should keep in mind that the main oxygen (bonding) states are situated at energies of about -7 eV. All upper panels display standard DFT results, U=0, while all lower panels show GGA+U results for U=5 eV.

shell of Co and will be discussed in the following section.

B. Ground states for Mn-, Fe-, Co-, and Ni-doped Cu₂O

In cuprous oxide a substituent (e.g. Co) on the Cu site has site symmetry D_{3d} ($\bar{3}m$). Thus the d orbitals can be characterized by two different irreducible representations, namely A_{1g} with $d_{2z^2-x^2-y^2}$ and E_g with ($d_{xy}, d_{x^2-y^2}$), respectively (d_{xz}, d_{yz}) as symmetrized basis functions. These functions are given in a coordinate system with the z axis pointing towards one of the two nearest neighbor oxygens. Thus we performed not only calculations for cubic $TM_1Cu_{31}O_{16}$ but also for equivalent trigonal cells ($R\bar{3}m$, No. 166), having a z axis

pointing along the cubic $(1,1,1)$ direction (see Fig. 1). These trigonal cells contain 18 atoms and the orbital projected DOS shown in Fig. 3 are useful for understanding the trends in bonding. In all calculations, relaxations of the atomic positions were allowed as long as symmetry was not reduced. The results for the magnetic moments determined for low TM concentrations (3.2%) as well as for high concentrations (9.1%) (given in brackets) are listed in Table II.

From the DOS in Fig. 3 one can see that for $Mn_1Cu_{11}O_6$ the Fermi energy E_f is situated (slightly) within the conduction band for the spin up electrons and within a gap for the spin down electrons. In the spin down channel the peak below E_f is predominantly composed of d_{z^2}-like states, with contributions of ($d_{xy}, d_{x^2-y^2}$). This peak originally comes

TABLE II. Magnetic moments in μ_B for 3.2% and 9.1% (in brackets) of transition metal (TM) substitution in Cu_2O, assuming TM to be situated on the Cu site. Listed are the total and site projected magnetic moments, the radii of integration were chosen to be $r=2.5$ bohr for TM and $r=1.55$ bohr for the oxygens (only those closest to the substituent were considered). The upper/lower part of the table is valid for $U=0$ eV/$U=5$ eV, respectively.

		Mn	Fe	Co	Ni
Moment ($U=0$ eV)					
Total	$[\mu_B/\text{cell}]$	4.02 (4.05)	3.00 (3.08)	2.00 (2.00)	1.00 (1.00)
on TM	$[\mu_B/\text{atom}]$	3.85 (3.73)	2.88 (2.87)	1.89 (1.90)	0.56 (0.57)
on O	$[\mu_B/\text{atom}]$	0.01 (0.02)	0.04 (0.04)	0.05 (0.05)	0.02 (0.03)
Moment ($U=5$ eV)					
Total	$[\mu_B/\text{cell}]$	4.34 (4.24)	3.07 (3.18)	2.00 (2.00)	1.00 (1.00)
on TM	$[\mu_B/\text{atom}]$	4.40 (4.29)	3.39 (3.28)	2.16 (2.11)	0.78 (0.76)
on O	$[\mu_B/\text{atom}]$	−0.01 (0.02)	0.02 (0.01)	0.02 (0.03)	−0.02 (0.01)

from Mn-O antibonding states that in pure Cu_2O are responsible for the uppermost peak in the Cu-d DOS at the valence band maximum (see Fig. 2). These antibonding states can be attributed rather to the Mn atom, and in a simple covalent bond picture (Cu_2O is not purely ionic) the electron on Mn (d_{z^2}) prefers being spin paired with the electron on oxygen that is in an orbital pointing towards Mn. Hence the d_{z^2} state does not contribute to magnetism, which can be seen in the DOS. Some of the spin-down d_{z^2}-like states (including the peak) are occupied, and compared to the undoped host the peak is shifted away by intraatomic exchange interactions from the valence band edge to slightly below E_f. If the Hubbard U is set to a value of 5 eV, minority ($d_{xy}, d_{x^2-y^2}$)-like states are no longer occupied and the number of Mn spin down d_{z^2}-like electrons also goes down. The peak itself is slightly shifted upwards. Regarding site-projected charges, within a radius r_{TM} of 2.5 bohr around Mn the number of minority electrons reduces from 0.6 for $U=0$ to approximately 0.3 for $U=5$ eV. The total d-like charge within this radius decreases slightly from 4.95 to 4.92 electrons. A Bader charge analysis for the present material using an algorithm of G. Henkelman *et al.*[21,22] results in a total charge on Cu of 10.5 ($s+d$), on O of 7.1 ($s+p$) and on Mn of 6.1 ($s+d$) electrons ($U=0$). In conclusion, the total magnetic moment of ≈ 4 μ_B can be explained by the fact that all orbitals except the d_{z^2} are spin polarized. The minority d_{z^2}-like states are emptied if on-site correlations beyond GGA are introduced (e.g., by U), causing an increase of the total and site-projected magnetic moment.

The one additional electron in $Fe_1Cu_{11}O_6$ goes into the ($d_{xy}, d_{x^2-y^2}$) orbitals, which are nonbonding with respect to the nearest neighbor oxygens. These orbitals spread out within the trigonal $z=0$ plane. The local coordination of the TM atom within this plane is a hexagon built up from six nearest neighbor Cu atoms and another hexagon (rotated by 30° with respect to the Cu hexagon) built up from second nearest neighbor oxygens, alternating above and below the $z=0$ plane. The magnetic moment is approximately 3 μ_B and changes slightly upon a change in the Fe concentration and moderately upon an increase in U. For the spin-up electrons, E_f is situated within the bottom of the conduction band and contrarily to the Mn compound spin-down E_f is situated

within the ($d_{xy}, d_{x^2-y^2}$)-like states (see Fig. 3), broadened by spurious TM-TM interactions due to the limited size of the supercell. The Bader charge for $U=0$ on Fe is 7.3 ($s+d$), larger by 1.2 compared to Mn. Also the total d-like charge within $r_{TM}=2.5$ bohr around Fe increases by 1.1 ($U=0$), indicating that the charge is slightly more localized on the Fe atom than it is on the Mn. When the total DOS of the 48 atom cubic supercells (not shown) is taken into consideration, one finds that the energetic position of the spin up conduction band is slightly higher in Fe- than in Mn-doped Cu_2O. If U is set to 5 eV, the spin up conduction bands (for the cases Mn and Fe) are clearly shifted downwards. This is similar to n-type doping, which usually shifts E_f inside the conduction band.

The situation changes significantly if one additional electron is present at the TM site. $Co_1Cu_{11}O_6$ is the first compound within the series exhibiting a stable integer magnetic moment of 2 μ_B. It has a vanishing DOS at E_f for both spin channels. Compared to the representatives discussed above, in the Co-doped system, E_f for spin up is no longer inside the conduction band. For the other spin channel, the antibonding d_{z^2} peak is occupied as well as a second set of orbitals, namely ($d_{xy}, d_{x^2-y^2}$). This allows E_f to be situated inside a crystal field gap, separating the occupied orbitals from the empty ones that have predominantly (d_{xz}, d_{yz}) symmetry. The Bader charge on Co is 8.4 ($s+d$) (for $U=0$), by 1.1 electron more than on Fe. This increase relative to the core charge reflects the increase in electronegativity when the d shell is being filled. The d-like charge within r_{TM} (2.5 bohr) is 7.23, which relative to the core charge is largest among all members of the series. In the previous section about relaxations it was found that the TM-TM and TM-O bond length are smallest for the Co-doped compound. This stronger binding may be attributed to E_f falling just inside a gap, which very often is energetically favored. Moreover, the approximately half-filled $d^{\downarrow}$ shell is also optimal for binding, because (for spin down) the energetically favored orbitals are occupied whereas the others are still empty. When the Hubbard U is increased, the local moment increases from 1.89 to 2.16 μ_B, and since the total moment does not change, the neighbors have to contribute antiferromagnetically to the total moment.

The compound $Ni_1Cu_{11}O_6$ is either half-metallic ($U=0$ eV) with a high DOS at E_f in the spin down channel, or

TABLE III. $\Delta E = E_{AF} - E_{FM}$ gives the energy differences in meV between AF and FM arrangement of two spins for interactions up to the fifth neighbor shell. The TM-TM distance in multiples of the fcc nearest neighbor distance is given in brackets in the head of the table. Positive values of ΔE indicate FM ordering. The magnetic moments are determined inside a sphere of 2.0 a.u. CE stands for clustering energy, which is the energy of a given atomic arrangement (2nd to 5th nearest neighbor position) relative to the ground state energy of a system with nearest neighbor TM substituents. Negative values indicate that the given configuration is lower in energy than the nearest neighbor reference.

			1st (1)	2nd ($\sqrt{2}$)	3rd ($\sqrt{3}$)	4th (2)	5th ($\sqrt{6}$)
Mn	$U=5$ eV	ΔE [meV]	−106	−70	−53	−53	−64
		Moment (FM/AF) [μ_B]	4.42/4.38	4.42/4.38	4.36/4.37	4.35/4.35	4.38/4.38
	$U=0$ eV	ΔE [meV]	−64	−59	−33	−1	−20
		Moment (FM/AF) [μ_B]	3.79/3.85	3.79/3.85	3.83/3.86	3.78/3.85	3.83/3.88
		CE [meV]		0	0	+34	+72
Co	$U=5$ eV	ΔE [meV]	−73	+1	+14	+3	−5
		Moment (FM/AF) [μ_B]	2.13/2.16	2.15/2.16	2.15/2.15	2.16/2.16	2.15/2.16
	$U=0$ eV	ΔE [meV]	+60	+47	+33	+7	−3
		Moment (FM/AF) [μ_B]	1.87/1.85	1.86/1.87	1.88/1.88	1.90/1.90	1.90/1.90
		CE [meV]		+2	+35	+110	+108

it has no states at E_f in both spin directions ($U=5$ eV). In both cases the total magnetic moment is integer 1, with a local moment of 0.56 and 0.78 for $U=0$ and 5 eV, respectively. The Bader charge of Ni for $U=0$ is 9.5, reflecting the fact that Ni has a similar tendency to fill its d shell (a similar electronegativity) as Cu with a Bader charge of 10.5 ($s+d$). The total d-like charge inside r_{TM} is 8.07 ($U=0$). A more detailed investigation of the DOS shows that for $U=0$ eV, the energetic sequence of d orbitals has changed compared to the compounds discussed earlier. Energetically lowest are ($d_{xy}, d_{x^2-y^2}$), followed by (d_{xz}, d_{yz}). The minority spin d_{z^2} peak is situated above E_f. This might come from the tendency of E_f being situated within a region of vanishing DOS. If the nondegenerate spin-down d_{z^2}-like peak were below E_f as for all the other representatives, the twofold degenerate set (d_{xz}, d_{yz}) would have to be half-filled and E_f would fall into a peak. Only in the Fe compound is E_f situated within a spin-down peak. This is because in that case the larger spin splitting makes a rearrangement of the spin down orbitals unfavorable. The Hubbard U further empties the d_{z^2}-like states, most probably due to Coulomb repulsion arising from the occupied (d_{xz}, d_{yz}) states.

Regarding structural properties, the contraction of the TM-O bond length when going from the Mn- to the Co-doped compound might originate from the fact that a half-filled $d^\downarrow$ shell is favored, since the bonding part is occupied and the unfavored states are empty. The position of E_f within a crystal field gap as in the case of the Co system is also favorable, explaining the exceptionally small Co-O bond length. When it comes to the magnetic properties, the earlier members of the series (Mn, Fe) are close to a half-metallic state, however, their total magnetic moment depends on the Hubbard U as well as slightly on the TM concentration (see Table II). This sensitivity is due to the fact that upon, e.g., an increase of U, it rather comes to an emptying of minority d states than to a rearrangement of occupied states as in the case of Co. Since approximately one d orbital (d_{z^2}) does not contribute to magnetism due to its strong overlap with non-

spin-polarized oxygen, the total moment for Mn- and Fe-doped Cu$_2$O is about 4 and 3 μ_B, respectively. The compounds containing Co and Ni are clearly either half-metallic (Co: $U=0/5$ eV, Ni: $U=0$ eV) or insulating (Ni, $U=5$ eV), meaning that there are no states at E_f in either one or even both spin directions. As one would expect, due to the filling of minority d states on TM the total magnetic moment is 2 and 1 μ_B for Co- and Ni-doped Cu$_2$O, respectively. If Cu is substituted by lighter transition metals, the lower electronegativity compared to Cu acts similar to n-type doping. The charge that cannot be localized is no longer spin polarized, explaining why for the spin up channel E_f is situated within the conduction band (Mn/Fe). By adding further electrons on TM, E_f then successively moves away from the spin-up conduction band, until it almost reaches the valence band edge in the case of Ni, which has an electronegativity similar to Cu.

C. Magnetic exchange in Co- and Mn-doped Cu$_2$O

In order to investigate the effective magnetic exchange between two substituents, the energy difference between a ferromagnetic (FM) and an antiferromagnetic (AF) spin arrangement for two TM atoms in TM$_2$Cu$_{30}$O$_{16}$ (6.7% doping rate) has been determined (Table III). One TM was put at the origin (0,0,0), the other one was assumed to occupy either the nearest neighbor ($\frac{1}{4}, \frac{1}{4}, 0$), the second nearest neighbor ($\frac{1}{2}, 0, 0$), the third nearest neighbor ($\frac{1}{2}, \frac{1}{4}, \frac{1}{4}$), the fourth nearest neighbor ($\frac{1}{2}, \frac{1}{2}, 0$), or the fifth nearest neighbor ($\frac{1}{2}, \frac{1}{2}, \frac{1}{2}$) positions, the fractional coordinates refer to the supercell. Again, geometric relaxations were taken into account. In order to analyze possible clustering, the energetically favored spin arrangement (AF or FM) has been recalculated without any symmetry-related constraints. This improves the total energy predominantly for the nearest neighbor arrangement, typically by several meV.

In the compound Co$_2$Cu$_{30}$O$_{16}$, FM alignment is favored up to the fourth nearest neighbor interaction, only the distant

fifth nearest neighbor interaction is weakly antiferromagnetic. An oscillatory behavior is found when correlations are switched on ($U=5$ eV). Since the on-site Coulomb repulsion directly influences only the local environment around Co, predominantly the shorter interactions are modified towards antiferromagnetic coupling. A very important fact is that the magnetic interactions decay rather rapidly when the distance between the Co substituents is increased, regardless of the strength of U. This suggests that magnetic exchange is not carrier mediated in $Co_2Cu_{30}O_{16}$, which is in good agreement with the DOS discussed in the previous section. The Fermi energy is situated clearly inside the host gap for the majority spin direction and inside a d band gap for the spin down electrons, which is stable against all values of U investigated. Thus no host states are available at E_F and long-range Zener p-d exchange[23] between well-localized magnetic moments, mediated by host hole states, is probably not responsible for magnetic exchange. The values of the clustering energies (CE) suggest that it is most favorable for Co to occupy nearest or next nearest neighbor sites, thus for the real Co-doped material, rather strong clustering can be expected if produced at too high temperatures where the mobility of the atoms is rather large. A comparison of the local magnetic moments at the substituents for the FM and AF configuration exhibits only minor differences.

In $Mn_2Cu_{30}O_{16}$, magnetic exchange is exclusively antiferromagnetic for all pairs of substituents investigated. When the Hubbard U is increased, the antiferromagnetic character becomes even stronger. This shows that ferromagnetism, which would be desirable for spintronics applications, is not an intrinsic property of this compound. The strength of the magnetic interactions decays much more slowly with increasing distance than for the Co-doped oxide, especially when correlations are introduced. Clustering is less pronounced than in the corresponding Co compound.

Both compounds have in common that there is a continuous change in the exchange constants between nearest neighbors and between impurities farther off. Since only the nearest and fourth nearest neighbor sites belong to the same Cu-O-Cu zigzag chain, which allows for an interaction of the substituents via the oxygens, indirect superexchange via the closed shell oxygen is not the only interaction present. This is obvious because the cation sublattice is of fcc type and a deviation from a d^{10} configuration in such a lattice introduces cation-cation bonding without the direct involvement of oxygen.

Due to the ongoing discussion about the realizability of room temperature ferromagnetism in Mn-doped cuprous oxide, we additionally took into account defects, which in a semiconductor are expected to play an important role. We assumed single copper as well as oxygen vacancies, the most relevant defects in Cu_2O.[24,25] For this purpose we removed one atom of our supercell [Cu at $\left(0, \frac{1}{4}, \frac{1}{4}\right)$ or O at $\left(\frac{1}{8}, \frac{1}{8}, \frac{1}{8}\right)$] and allowed for a relaxation of all other atoms but with a fixed lattice constant. All calculations were performed applying GGA only ($U=0$). Our results are shown in Fig. 4, presented together with the exchange constants of the defect-free oxide discussed above.

On the left-hand side, the results for Mn-doped Cu_2O clearly show that both copper and oxygen vacancies strongly
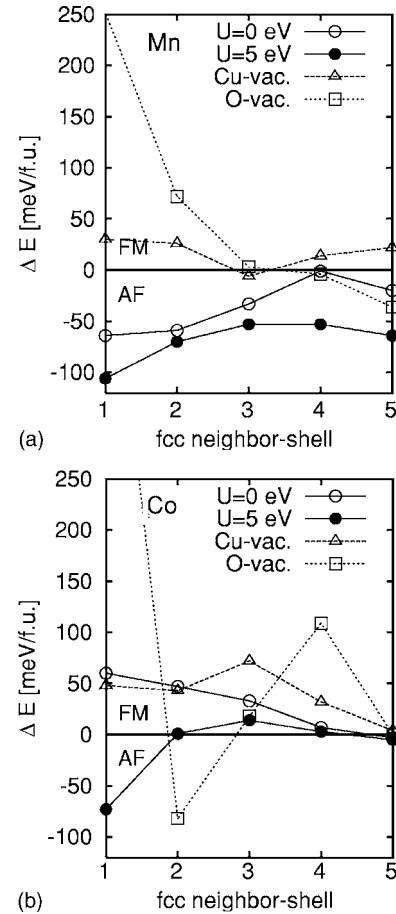
FIG. 4. Energy difference in meV between AF and FM coupling (E_{AF}-E_{FM}) as a function of fcc neighbor-shell distance. The solid lines show the data for Mn (left-hand side) and Co (right-hand side) doping of perfect Cu_2O, the dashed lines represent Mn/Co doping of Cu_2O exhibiting intrinsic defects, such as copper vacancies (Cu-vac.) and oxygen vacancies (O-vac.).

enhance the FM character of the Mn-Mn interactions. However, while Cu vacancies cause Mn to couple predominantly FM, except for a small AF third nearest neighbor interaction, the effect of oxygen vacancies is more complex. Even though the removal of oxygen affects magnetic exchange more strongly (e.g., huge Mn-Mn nn interaction of 252 meV), Fig. 4 indicates that the Mn-Mn interactions in this case change sign towards AF coupling with increasing TM-TM separation. Due to the limitation of the supercell size we can only estimate the behavior of Mn-Mn pairs farther off, but further AF interactions can be expected. Thus it is not clear which type of defect is suited best for achieving a T_c as high as possible, however, the important finding is that defects, regardless whether oxygen or copper vacancies, are an important ingredient to stabilize FM Mn-Mn interactions.

In the Co-doped system, oxygen vacancies again have a much stronger influence on magnetism. While Cu holes slightly stabilize FM interactions, O holes induce extremely strong oscillations, which are not desirable for long-range FM. As a consequence, in this system one can expect that Cu holes, which might appear under Cu-poor preparation condi-

tions, increase the Curie temperature. Contrarily, the lack of oxygen and the resulting short-ranged oscillations in the Co-Co magnetic interaction might be one prerequisite for the spin-glass behavior in Co-doped Cu_2O found in experiment.[4]

To summarize, cuprous oxide Cu_2O with transition metals substituted on the copper site exhibits a great variety of magnetic ground states. Ni and Co substitution introduces stable integer magnetic moments per cell, and thus results in either insulating (Co, Ni $U=5$ eV) or half-metallic (Ni $U=0$) ground states. In semimetallic, defect-free $Mn_2Cu_{30}O_{16}$, independently of U, antiferromagnetic spin arrangement is favored. Long-range ferromagnetism might occur when defects (copper or oxygen vacancies) are present. The huge difference between the magnetic properties of perfect and imperfect Cu_2O resolves the discussion about room temperature

ferromagnetism, and explains why some groups find long-range FM and others not. On the other hand, in insulating defect-free $Co_2Cu_{30}O_{16}$, most of the exchange constants already favor ferromagnetism, only the exchange between nearest neighbor sites changes toward an AF coupling when the Hubbard U is increased. When defects are taken into account, it turns out that copper vacancies are very likely to increase T_c while a lack of oxygen introduces strong oscillations in the magnetic exchange, favoring a more complex type of ordering. This is in fair agreement with experiment, which even suggests spin-glass behavior in Co-doped Cu_2O, if no additional Al doping is performed. Our calculations further revealed that magnetic interactions are relatively short ranged in the Co-doped system but longer ranged in the Mn-doped compound.

[1] M. Wei, N. Braddon, D. Zhi, P. A. Midgley, S. K. Chen, M. G. Blamire, and J. L. MacManus-Driscoll, Appl. Phys. Lett. **86**, 072514 (2005).

[2] L. Pan, H. Zhu, C. Fan, W. Wang, Y. Zhang, and J. Q. Xiao, J. Appl. Phys. **97**, 10D318 (2005).

[3] M. Ivill, M. E. Overberg, C. R. Abernathy, D. P. Norton, A. F. Hebard, N. Theodoropoulou, and J. D. Budai, Solid-State Electron. **47**, 2215 (2003).

[4] S. N. Kale, S. B. Ogale, S. R. Shinde, M. Sahasrabuddhe, V. N. Kulkarni, R. L. Greene, and T. Venkatesan, Appl. Phys. Lett. **82**, 2100 (2003).

[5] A. Martinez-Ruiz, M. G. Moreno, and N. Takeuchi, Solid State Sci. **5**, 291 (2003).

[6] G. Kresse and J. Furthmueller, Phys. Rev. B **54**, 11169 (1999).

[7] G. Kresse and J. Joubert, Phys. Rev. B **59**, 1758 (1999).

[8] W. Kohn and L. J. Sham, Phys. Rev. **140**, A1133 (1965).

[9] J. Perdew, K. Burke, and M. Ernzerhof, Phys. Rev. Lett. **77**, 3865 (1996).

[10] S. L. Dudarev, G. A. Botton, S. Y. Savrasov, C. J. Humphreys, and A. P. Sutton, Phys. Rev. B **57**, 1505 (1998).

[11] A. P. Young and C. M. Schwartz, J. Phys. Chem. Solids **30**, 249 (1969).

[12] H. D. H. A. Werner, Phys. Rev. B **25**, 5929 (1982).

[13] J. Ghijsen, L. H. Tjeng, J. van Elp, H. Eskes, and M. T. Czyzyk, Phys. Rev. B **38**, 11322 (1988).

[14] R. Laskowski, P. Blaha, and K. Schwarz, Phys. Rev. B **67**, 075102 (2003).

[15] L. E. Orgel, J. Chem. Soc. **1958**, 4186.

[16] P. Marksteiner, P. Blaha, and K. Schwarz, Z. Phys. B: Condens. Matter **64**, 119 (1986).

[17] L. Kleinmann and K. Mednick, Phys. Rev. B **21**, 1549 (1980).

[18] E. Ruiz, S. Alvarez, P. Alemany, and R. A. Evarestov, Phys. Rev. B **56**, 7189 (1997).

[19] W. Y. Ching, Y.-N. Xu, and K. W. Wong, Phys. Rev. B **40**, 7684 (1989).

[20] H. Kikuchi and K. Tonooka, Thin Solid Films **486**, 33 (2005).

[21] R. Bader, *Atoms in Molecules: A Quantum Theory* (Oxford University Press, New York, 1990).

[22] G. Henkelman, A. Arnaldsson, and H. Jonsson, Comput. Mater. Sci. **36**, 254 (2006).

[23] T. Dietl, H. Ohno, and F. Matsukura, Phys. Rev. B **63**, 195205 (2001).

[24] R. Haugsrud and T. Norby, J. Electrochem. Soc. **146**, 999 (1999).

[25] O. Porat and I. Riess, Solid State Ionics **74**, 229 (1994).